

An analysis of multi objective energy scheduling in PV-BESS system under prediction uncertainty

Unnikrishnan Raveendran Nair, Monika Sandelic, Ariya Sangwongwanich, Tomislav Dragičević, *Member, IEEE*, Ramon Costa-Castelló, *Senior, IEEE*, and Frede Blaabjerg, *Fellow, IEEE*

Abstract—Energy storage systems (ESS) are being considered to overcome issues in modern grids, caused by increasing penetration of renewable generation. Nevertheless, integration of ESS should also be supplemented with an optimal energy management framework to ensure maximum benefits from ESS. Conventional energy management of battery, used with PV system, maximises self-consumption but does not mitigate grid congestion or address battery degradation. Model predictive control (MPC) can alleviate congestion and degradation while ensuring maximum self-consumption. Studies will be carried out to highlight the improvement with MPC based energy management over conventional method using simulations of one-year system behaviour. As MPC uses forecast information in decision making, the impact of forecast uncertainties will be assessed and a method to address them through a constraint tightening will be presented.

I. INTRODUCTION

RENEWABLE sources (RES) in electric grids are environment friendly but tend to not be grid friendly. The intermittent nature of this generation has led to grid congestions, voltage regulation problems and instabilities [1]. Energy storage systems (ESS) are increasingly utilised to overcome these issues and facilitate the RES integration [2]. However, they need to be managed optimally. The need for optimal management is highlighted through a PV system with battery energy storage system (BESS). As grid parity is achieved in PV generation [3] economically consumer benefit by maximising self consumption. The conventional methods achieves the same by charging the BESS whenever surplus PV power is available. In days of high PV generation this leads to BESS being fully charged early in the day. As a result when peak PV generation occur the surplus power is fed to grid. This severely congest grid when multiple PV units do the same and there is no sufficient load demand. As a result, nowadays feed-in power limitations are being imposed in PV systems to avoid congestions [3], which also limiting RES power utilisation.

Another drawback with conventional maximising self consumption strategy is the BESS degradation. The two major ageing mechanism in BESS (Li-ion based) are the cyclic and calendar ageing. They are results of degradation arising from excessive cycling of BESS and increased dwell time at high SOC levels. In conventional scheme the early charging of

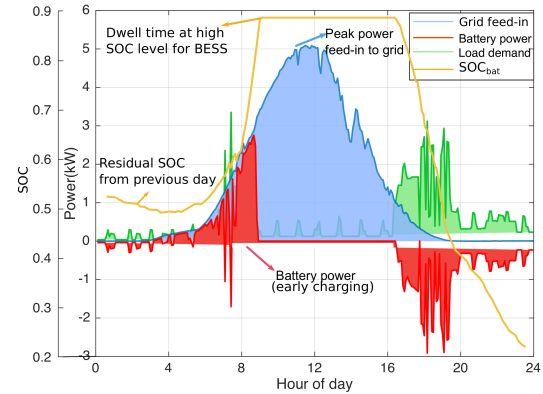


Fig. 1: Typical BESS charging, SOC and grid feed-in profile under maximising self consumption strategy. Early full charging of BESS and subsequent peak power feed-in observed.

BESS results in high SOC dwell periods (Fig.1) and increased BESS degradation [4], [5].

Forecast based BESS management techniques can overcome this issue and provide better performance. The knowledge of future generation and load profiles allow energy management (EM) systems to know the instance of peak PV generation. This facilitates prevention of early full-charging by BESS and ensures BESS capacity is available during peak PV generation. This can limit the feed-in power to grid and address the grid congestion. Therefore, forecast based energy scheduling can handle multiple objectives while making decision (typically addressed using optimisation problems) [6], [7]. In forecast based energy scheduling for PV-BESS system, offline approaches has been explored in [8], [9]. However, these approaches tend to have increased dependencies on real-time controllers to compensate for prediction error, resulting in sub-optimal system behaviour.

Online forecast based scheduling using model predictive control (MPC) can ensure better performance over the offline techniques [10], [11]. MPC for optimal energy scheduling has been explored [6], [12] with promising results, but mostly for minimising operating costs in electric grids. An application of the same to address issues like grid congestion, BESS degradation or self consumption, as highlighted in the PV BESS system, has not been carried out. Different techniques have been developed to account for the uncertainty in prediction [10], [13] but they result in conservative decision making by the MPC. If not formulated properly, these methods can over compensate for prediction errors, resulting in poor performance.

In this work, the application of MPC in a PV-BESS sys-

Dr. Nair. and Dr. Costa-Castelló were with the Universitat Politècnica de Catalunya (UPC)

This work was supported in part by the Spanish Ministry of Economy and Competitiveness under Projects CICYT RTI2018-094665-B-I00, DOVELAR ref. RTI2018-096001-B-C32 (MCIU/AEI/FEDER, UE) and María de Maeztu Seal of Excellence to IRI (MDM-2016-0656), and by the Generalitat de Catalunya through the Project 2017 SGR 482.

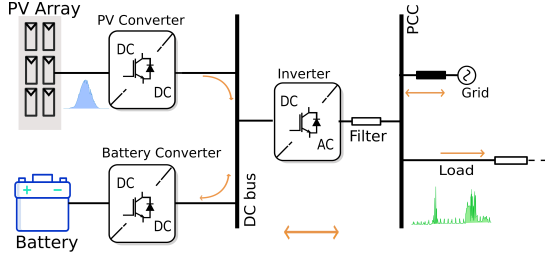


Fig. 2: Schematic of the test case microgrid .

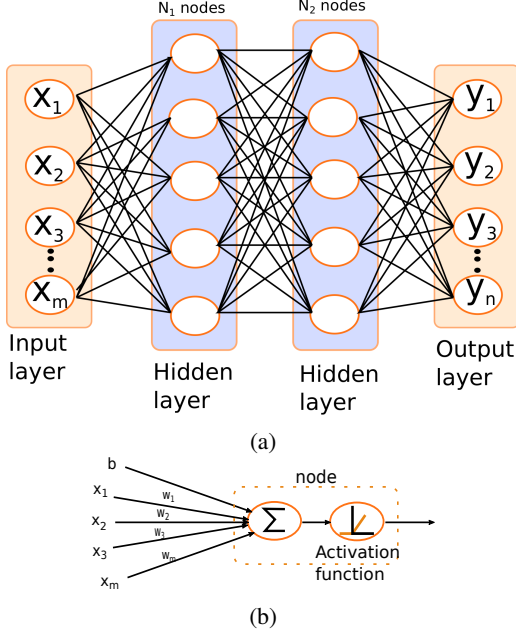


Fig. 3: (a) Feedforward neural network structure used in forecasting unit, (b) node representation.

tem to address multiple objectives like maximising self consumption, minimising grid congestion and BESS degradation is considered. The proposed work will present a complete predictive EM scheme which involves a forecasting unit and MPC for BESS scheduling. This work also addresses the issue of uncertainty in prediction through utilisation of a simple constraint tightening approach. One of the objective will be to quantify how performance objectives will be affected by the uncertainty handling. The economic and electrical aspects of PV BESS system operation will be considered, using simulated results of one year energy scheduling. As far as the authors' knowledge goes such an application of MPC in PV-BESS system and the assessment of the impact of decision making accounting for prediction uncertainty have not been carried out before.

The rest of the paper is organised as follows. Section II introduces the predictive energy management scheme (PEMS) with the forecasting stage and MPC based scheduling. Section III presents the result of PV-BESS scheduling with the PEMS and quantifies the improvements achieved with the same. Finally the work is concluded in Section IV.

II. PREDICTIVE ENERGY MANAGEMENT SCHEME

The PV-BESS system considered in this work is shown in Fig.2. The predictive EM scheme implemented comprises of

two stages, the Forecasting unit and the MPC based scheduling unit.

A. Forecasting unit

This section will focus on how a forecasting system can be integrated with a predictive energy management system (PEMS). As such a neural network (NN) [14] based forecasting system will be considered in this work. Recent works have demonstrated that NN based machine learning models are capable of improved prediction of PV generation [15], load demand [16] especially on localised load forecasting [17], as considered in this work.

A typical NN framework is shown in Fig. 3(b). It consists of an input layer, two hidden layers and an output layer. The two hidden layers have N_1 and N_2 nodes respectively. The structure of each node is shown in Fig. 3(b). The NN shown here is fully connected, meaning that each node receives input from all the nodes in the previous layer scaled by a weighting factor (w_k) along with a biasing factor b , as shown in Fig.3. The activation function considered at each node is a rectified linear unit (ReLU) as shown in Fig. 3(b). The ReLU is used as it is considered to provide an improved performance [18].

In order to obtain highly accurate predictions on generation or load profiles from the NN system, they need to be trained using the previous sampled data of the same. The training process can be considered as a learning phase of the NN, wherein the previous generation and load data is used by the NN to study the underlying behavioural pattern. This knowledge will then be used by the NN to define the optimal values for the weighting and biasing factors, so that NN can start predicting future generation and load behaviour with high accuracy. The mathematical formulations involved in the training process and the related algorithms [19] are beyond the scope of this work.

B. MPC based scheduling unit

MPC is a modern optimal control strategy which enables handling of non linearities and constraints efficiently [10]. In EM problems economic MPC is typically considered [10]. The MPC uses predicted value of generation, load profiles and an appropriate system model to predict evolution of system states into a future predefined time period called the control horizon. Using online optimization, MPC will modify the manipulated inputs so that the system states will follow an optimal trajectory in this horizon. This in-turn will guarantee that the system behaviour is optimised w.r.t.o some predefined performance parameters.

At any sampling instant, k , for a control horizon N , the MPC generates N set-points ($s_{0|k}, s_{1|k}, s_{2|k}, \dots, s_{N-1|k}$) where $s_{i|k} = s(k+i) \quad \forall i = 0, 1, 2, \dots, N-1$. The first set-point, $s_{0|k}$, will then be applied to the system. This process is repeated at every sampling instant using the sampled value of system states at that moment. This ensures that the control action is generated using latest system states, thus giving a sense of feedback [10], [13]. The formulation of the optimisation problem used in MPC for EM of PV BESS system is discussed next.

1) *Cost function:* The cost function

$$J(k) = \min \sum_{i=k}^{k+N-1} (J_{\text{grid}}(i) + J_{\text{bess}}(i)). \quad (1)$$

defines the aspects of PV BESS system operation. There are two parts to the above cost function. The first part J_{grid} is defined as

$$J_{\text{grid}}(i) = \lambda_g \cdot p_{\text{grid}}(i)^2 \quad (2)$$

where λ_g is a penalising weight. The above cost term penalises the power interaction with the grid (p_{grid}). As a result, if (1) is to be minimised the EM scheme will try to keep the values of p_{grid} as low as possible. This will ensure that grid feed-in is reduced. By ensuring that grid feed-in minimised, the MPC indirectly forces the generated PV power to be utilised, as far as possible. This increases self consumption.

The second term in (1), given by

$$J_{\text{bess}}(i) = \lambda_s \cdot \text{SOC}(i)^2 + \lambda_d \cdot \Delta \text{SOC}(i)^2 \quad (3)$$

minimises battery degradation. λ_s, λ_d are weighting factors. As mentioned before, in Li-ion batteries, the calendar, cycling ageing are accelerated through high SOC dwell times and excessive cycling respectively. These effects are minimised through (3). In (3) SOC penalises high SOC values, thereby minimising highly charged states in BESS for longer duration. The ΔSOC in (3) penalises change in SOC and thereby excessive cycling. The explicit equation defining the battery degradation is not considered here as it is non-linear [4]. This can lead to increased complexity in solving the optimisation problem [20]. The quadratic functions, shown above provides a reasonable approximation which can be efficiently solved

2) *BESS model:* MPC used ESS and grid models during the optimization. The BESS model is based on the Coulomb counting equation given by

$$\text{SOC}(i+1) = \text{SOC}(i) - \frac{T_s}{C_{\text{bess}}} \cdot p_{\text{bess}}(i) \quad (4)$$

where T_s is the sample period, $p_{\text{bess}}(i)$ is the power set point and C_{bess} is the capacity of BESS.

3) *Grid model:* The grid is modelled using the power balance equation as follows:

$$p_{\text{bess}}(i) + p_{\text{gen}}(i) + p_{\text{grid}}(i) - p_{\text{load}}(i) = 0 \quad (5)$$

where $p_{\text{grid}}(i)$ is the power exchanged with the grid, $p_{\text{gen}}(i), p_{\text{load}}(i)$ are the power generated by the RES and load demand respectively at time instant i .

4) *Constraints:* The problem constraints address physical limits of ESS and power limits of the power converter. These constraints are ensured by

$$p_c^{\min} \leq p_{\text{bess}}(i) \leq p_c^{\max} \quad (6)$$

where p_c^{\min} and p_c^{\max} are maximum power handling limits of the bidirectional converters of BESS.

The physical limits of BESS are addressed through

$$\text{SOC}^l \leq \text{SOC}(i) \leq \text{SOC}^u \quad (7)$$

where SOC^l is the lower bound and SOC^u is the upper bound on SOC of BESS. These bounds also protect from

degrading stress arising from high charged or deep discharged states of BESS. Introducing hard constraints like (7) can cause non-convergence of the optimisation problem. This can be overcome by using soft constraints [21]. The soft constraints allow some violation in the bounds on SOC, but improves the convergence of the optimisation problem. The (7) represented as soft constraints is given by

$$\text{SOC}^l - \epsilon_{\text{bess}} \leq \text{SOC}(i) \leq \text{SOC}^u + \epsilon_{\text{bess}} \quad (8)$$

where ϵ_{bess} are the slack variable which indicates the constraint violation. In order to ensure that the SOC limits are not significantly violated, the slack variables are penalised using a cost function like

$$J_{\text{soft}} = \lambda_\epsilon \cdot \epsilon_{\text{bess}}^2. \quad (9)$$

Therefore, the final optimisation problem used for set-point generation by MPC is summed up as

$$J = \min \sum_{i=0}^{N-1} (J_{\text{grid}}(i|k) + J_{\text{bat}}(i|k) + J_{\text{soft}}(i|k)) \quad (10)$$

subject to

$$\begin{aligned} &\text{ESS and Grid models (4), (5)} \\ &\text{Constraints (8), (6).} \end{aligned} \quad (11)$$

The above represents a quadratic programming problem which can easily be solved with solvers like Gurobi [22].

The optimal behaviour with predictive management unit relies on the accuracy of the forecast. A proper training of NN based forecasting unit can reduce, but not eradicate it. Therefore to account the same, the optimisation problem in MPC needs modification. In this context, a simple constraint tightening approach can ensure this [23].

In PV-BESS system, the critical information that the MPC needs from forecast is the total imbalance energy in a control window and the instance of peak imbalance power (peak generation). This enables decision on the degree of utilisation of BESS and when to deploy BESS charging/discharging to prevent grid congestion. The forecasting unit can give a fairly accurate indication of the peak generation periods (highlighted in the next section). However, errors exist in the predicted total imbalance energy in a control window.

The forecast at any instant is not definitive but vary within a certain bound $d_{i|k}$ defined as

$$d_{i|k} = \begin{cases} 0, & \text{for } i = 0 \\ [+ \Delta \theta_i, - \Delta \theta_i], & \text{for } i = 1, 2, \dots, N-1. \end{cases} \quad (12)$$

At the sampling instant k the actual value is known from sampled data, hence $d = 0$ at $i = 0$. As for the other points in the control horizon, $d_{i|k}$ should be accounted by MPC in decision making. In constraint tightening, this is achieved by modifying the bounds of the constraints, (11), in the optimisation problem. In BESS this will modify the SOC limits, thus ensuring that there is always some buffer capacity to accommodate for the prediction error. Defining $p_{\text{grid}}(i|k) - p_{\text{load}}(i|k)$ as $p_{\text{def}}(i|k)$, the predicted deficient power in the system, (5) is rewritten under prediction uncertainty as

$$p_{\text{bess}}(i|k) + p_{\text{gen}}(i|k) + u_{(i|k)} + p_{\text{def}}(i|k) + d_{(i|k)} = 0. \quad (13)$$

In the above equation additional term $u_{i|k}$ is the control action from the low-level controllers to counteract the uncertainty in forecast $d_{(i|k)}$. The predictive management unit bases its decision on the forecast value $p_{\text{def}(i|k)}$ which is the deterministic part of the imbalance forecast. Therefore (5) is split into deterministic part catered by the PEMS

$$p_{\text{bess}(i|k)} + p_{\text{gen}(i|k)} + p_{\text{def}(i|k)} = 0. \quad (14)$$

and uncertain part catered by low-level controller.

$$u_{(i|k)} = -d_{(i|k)}. \quad (15)$$

This requires that the bounds (8) and (6) be modified to ensure sufficient margin is available for the low-level control to counteract $d_{(i|k)}$. The power bounds, (6), are modified using (15) as

$$p_{\text{bess}}^{\min} + u_{(i|k)} \leq p_{\text{bess}(i|k)} \leq p_{\text{bess}}^{\max} - u_{(i|k)}. \quad (16)$$

leaving some margin for the low-level controller to modify the power setpoints from predictive management unit to account for $d_{(i|k)}$ without exceeding power limits.

In order to modify the SOC bounds (8) the BESS model (4) is represented using $u_{i|k}$ under uncertainty in forecast as

$$\begin{aligned} SOC(i+1|k) &= SOC(i|k) - \\ &\frac{T_s}{C_{\text{bess}}} \cdot (p_{\text{bess}(i|k)} + u_{(i|k)}) \end{aligned} \quad (17)$$

under assumption that $d_{(i|k)}$ is always catered by BESS until fully charged/discharged. This ensures maximum self consumption as well. The above is rewritten in terms of sampled SOC value at instant k ($SOC_{\text{bess}(0|k)}$) as

$$\begin{aligned} SOC(i+1|k) &= SOC(0|k) - \\ &\frac{T_s}{C_{\text{bess}}} \cdot \sum_{l=0}^i (p_{\text{bess}(l|k)} + u_{(l|k)}). \end{aligned} \quad (18)$$

The deterministic part in the above equation is

$$SOC(i+1|k) = SOC(0|k) - \frac{T_s}{C_{\text{bess}}} \cdot \sum_{l=0}^i (p_{\text{bess}(l|k)}) \quad (19)$$

and

$$\frac{T_s}{C_{\text{bess}}} \cdot \sum_{l=0}^i u_{(l|k)} = dx_{(i|k)} \quad (20)$$

forms the non deterministic part. Based on this, constraint tightening of (8) is done as follows

$$\begin{aligned} SOC^l - \epsilon_{\text{bess}} + dx_{(i|k)} &\leq SOC(i) \\ &\leq SOC^u + \epsilon_{\text{bess}} - dx_{(i|k)}. \end{aligned} \quad (21)$$

Finally the optimisation problem can be reformulated as

$$\min \sum_{i=0}^{N-1} (J_{\text{grid}(i|k)} + J_{\text{bat}(i|k)} + J_{\text{soft}(i|k)}) \quad (22)$$

subject to

$$\begin{aligned} \text{ESS and Grid models (19), (14)} \\ \text{Constraints (21), (16)} \end{aligned} \quad (23)$$

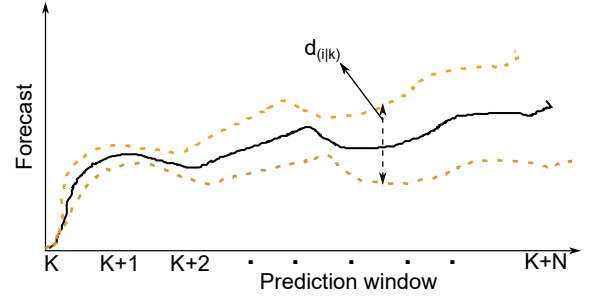


Fig. 4: Depiction of error propagation along forecast window.

Another important factor in defining the optimality of the solution is the size of $\Delta\theta$. A higher value of the same causes higher tightening of constraints and more conservative decision making. This prevents the BESS from charging or discharging too much, leading to low self consumption as the PV power being sent to grid and low self-consumption. In a site level system, like the PV-BESS of this work, the intraday variations in the load/generation profile tends to be high in comparison to an aggregated system. Forecasting the behaviour of such systems is always a tough problem as shown in [24]. In this scenario, defining $\Delta\theta_i$ based on a mean average error for every point in a prediction horizon leads to larger bounds $d_{(i|k)}$. However, if the error is aggregated over a forecast window there will be cancellation of error along the prediction window. This can result in a less conservative definition of error bounds if this mean absolute aggregate error, e_a , is taken to define $d_{(i|k)}$.

The distribution of e_a along $d_{(i|k)}$ can be done based on behaviour of forecasting unit. The initial values in any prediction window is highly correlated with the previous compared to latter values. As such the errors in forecast of initial values will be lower. Therefore, distribution of e_a in an increasing manner along a prediction horizon, as shown in Fig.4, to define $d_{(i|k)}$ makes practical sense.

C. Grid feed in limitation

To mitigate grid congestion from high surplus PV power feed-in restriction are imposed by utility operators. An example, is the case in Germany where PV systems with a power rating less than 30kW have to limit their feed in at 70% of their nominal value [25]. This condition can be easily implemented with MPC through constraints on p_{grid} . However, to ensure recursive feasibility an additional term will be introduced in (14) to define the power curtailment. This term will then have to be appropriately penalised in the cost function (22) to ensure that sub-optimal results do not occur. The additional decision variable for power curtailment will increase the computational demand of MPC. Therefore to overcome this issue, the optimisation problem will be solved as in (22) with (23) and the low-level controllers will ensure the power curtailment.

The entire PEMS for the PV-BESS with real-time control unit is shown in Fig. 5. This presents a hierarchical control scheme.

III. RESULTS AND DISCUSSION

The PV generation and load demand are emulated using one year's data from a test microgrid in Lindenberg, Germany

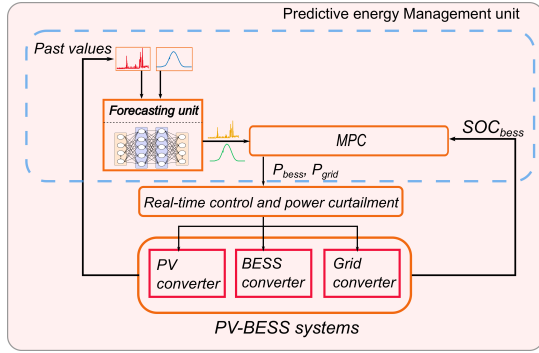


Fig. 5: Flowchart for the energy management decision making process, using predictive control, for PV BESS system.

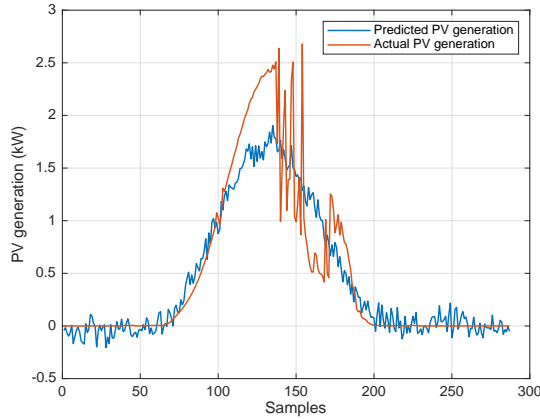


Fig. 6: Result of one day's PV generation forecast using NN on testing data. The data from 12 October 2004.

[26]. The load represents a four person household with annual demand of 4.5 MWh. The data was obtained using a sampling frequency of 5 minutes resulting in 288 samples a day. The sizing of the BESS system is done using the method highlighted in [3].

In this work, considering the daily cyclic behaviour of the PV-BESS system, the control horizon in MPC (N) was chosen as 24 hours. Therefore, objective of the forecasting unit at any instant will be to predict the next 24 hours.

A. Forecasting unit results

The NN was realised in Python using the Keras package [27]. Training was done with the ADAM solver [28]. In order to avoid overfitting of data cross validation and early stopping [29] was ensured during the NN training. One year's data was available of which 70% was used for training and remaining for testing in both PV and load forecast.

The NN input, used in PV forecast, was the last 72 hours of actual generation data. The 72 hour window was utilised considering the correlation of the PV generation to previous values. The 72 hour data also gives an indication of any existing weather conditions like, consecutive rainy days. Explicit weather data was not available and hence was not used as input to NN. This resulted in a NN with input layer size of $864 (288 \cdot \frac{72}{24})$. The hidden layer size, N_1 and N_2 , was chosen as 300 through multiple trials.

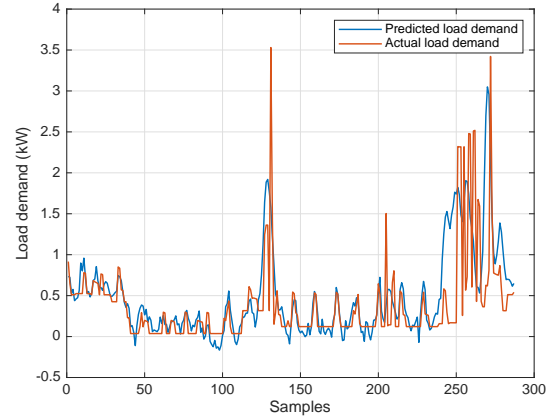


Fig. 7: Result of load demand forecast using NN.

The PV generation forecast with NN for a 24 hour period is provided in Fig.6. The forecast shown here is during autumn where, the solar irradiation and hence the generation tends to be lower. The usage of previous' days data as input for NN allows it to predict the low generation from seasonal effect. Nevertheless, it should be noted that the PV forecast is able to predict the time period where high generation occurs which is vital for the predictive management unit decision making.

The NN for the load forecasting used the last 168 hours (1 week) measured load demand as input. Unlike PV forecast, the one week data was used since the load demand on any day had high correlation with last weeks load demand on same day. This resulted in an input layer size of 2016 ($288 \cdot 7$) for NN forecasting load demand. The size of N_1 and N_2 was 300 chosen through multiple trials with trade off between accuracy and computational requirement. The results using the same for load forecast for a 24 hours period is shown in Fig. 7.

The PV and load forecast results highlight the difficulty in site level prediction (small systems), as discussed before. As shown in Fig.6 and Fig.7, the real data has sudden variations and the forecasting units could not entirely reproduce them. This justifies the importance of using mean aggregate absolute error to define $d_{(i|k)}$ as discussed before. In the PV data the average energy in a prediction window (moving window considered for MPC) was 13.56 kWh. The mean aggregate absolute error in the prediction window for the same is 3.28 kWh which was 23% the average energy value. Similarly, for the load prediction average energy in a prediction window was 10.81 kWh whereas the mean aggregate absolute error for the same was 1.015 kWh which was 9.3% the average energy value. The higher error with PV forecast is mainly due to lack of weather data.

The power deficiency profile ($p_{\text{def}(i|k)}$), used in MPC, was obtained from PV and load forecast. The individual aggregated error of PV and load forecast was also used to determine e_a .

B. Predictive energy management

The EM in the PV-BESS system will be carried for one year. The results from annual scheduling enables quantification of the long-term improvements that can be achieved with PEMS. The parameters used in the optimisation of the PEMS is shown in Table. I. Prior to presenting the results some performance

TABLE I: System parameters and their values used for the energy management strategy.

Parameter	Value
C_{bess}	9.375 kWh
Sampling time	5 min
MPC horizon (N)	24 hours
p_c^{min}, p_c^{max}	3 kW
SOC^u, SOH_{bess}^l	0.9, 0.1
$\lambda_g, \lambda_s, \lambda_d$	500, 3, 200

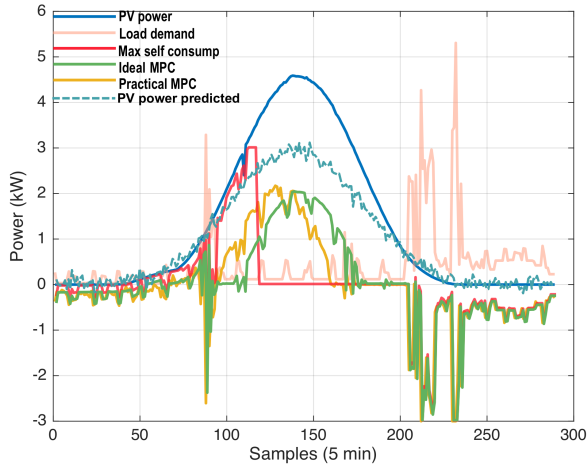


Fig. 8: Typical daily BESS power profiles with the different energy management strategies. The early full charging of BESS with the conventional method is overcome with PEMS.

measures will be introduced. An important measure that will be analysed is the self consumption ratio (SCR). SCR defines the percentage of total PV generation used by the microgrid system to meet its load demand (including energy storage in BESS). This is defined as

$$SCR = \frac{EPV_{consumed}}{EPV_{generated}} \cdot 100(\%) \quad (24)$$

where $EPV_{consumed}$ is the annual PV energy utilised by the consumer and $EPV_{generated}$ is the total annual PV energy generated. Another measure of interest will be the annual BESS degradation resulting from the EM strategy. The BESS profile generated from the EM strategy will be used in a BESS degradation model defined in [4] to assess the degradation.

The Fig.8 shows BESS charging profile in a 24 hours period with different strategies namely: the conventional maximising self consumption method, an ideal predictive management (ideal MPC) where perfect forecast of generation, load profile exists and the PEMS with constraint tightening (Practical MPC). The penalising weights $\lambda_g, \lambda_s, \lambda_d$ was chosen such that the SCR is the highest possible with minimum degradation. Unlike conventional method, in PEMS, BESS does not undergo early charging as shown in Fig.8. The charging of the BESS is shifted to period of higher generation. Comparing the ideal and practical MPC performance it can be observed that the BESS charging profile is shifted to an earlier instance when uncertainty exist. In the result shown in Fig.8, the predicted generation was lower than that of the actual

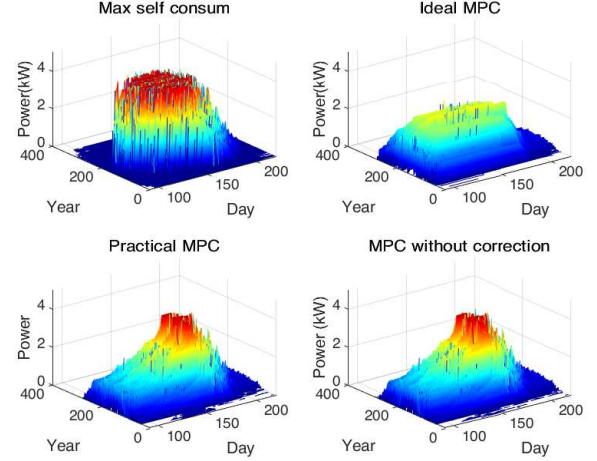


Fig. 9: Grid power feed-in profiles with different energy management schemes.

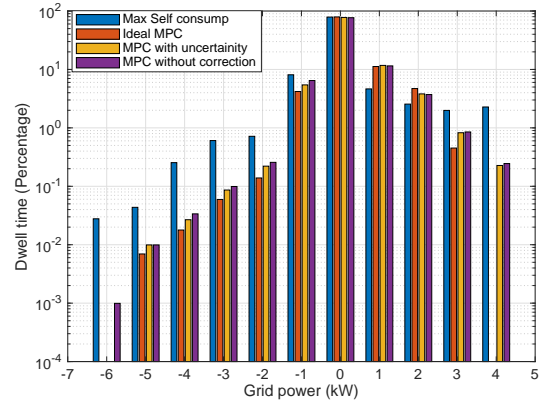


Fig. 10: Dwell times of power levels exchanged with the main grid under the different energy management schemes.

generation. This forced the practical PEMS to charge the BESS earlier than in the ideal case. Despite this the BESS charging was closer to the peak generation period in the practical case, in comparison to the conventional scheduling strategy.

The grid feed-in profiles are shown in Fig.9. The results shown here is after grid power feed-in curtailment (70% of the nominal value). In the conventional maximising self consumption method the early BESS charging results in peak power injection to grid as expected. The feed-in curtailment minimises the impact of this injection but at the cost of lesser utilisation RES generation. In the ideal MPC, as shown in Fig.9 this is completely mitigated with the perfect knowledge of future generation and load demand. In the case of practical MPC, the BESS reached full charge earlier than ideal MPC as shown in Fig.8. This leads to a small period of peak power injection to grid as shown in Fig.9. It should be noted that even with forecast errors the time duration of peak power injection in PEMS is significantly smaller than the conventional method

This is further highlighted in Fig.10 which shows the dwell times at different grid feed-in power levels. The PEMS with uncertainty in prediction shows lower dwell time at high feed-in power levels ($> 3kW$) compared to conventional

TABLE II: Comparison of SCR, BESS degradation and annual power curtailment for the different scheduling methods.

Scheduling method	Annual SCR (%)	Annual BESS degradation (%)	Annual PV power curtailed (kW)
Conventional method	54.6	3.94	542.5 kW
Ideal MPC	54.3	3.71	0
Practical MPC	52.71	3.73	35.91 kW
MPC without correction	52.73	3.65	37.83 kW

maximising self consumption scheme.

1) *Self-consumption ratio assessment*: The assessment of PV power self consumption is shown in Table.II, where annual SCR with different scheduling methods are compared. Considering a particular BESS sizing, the maximum SCR of 54.6% was observed in conventional maximising self consumption method. The SCR with ideal MPC is 54.32% which is 99.5% of the conventional scheme. The slight drop in self consumption is attributed to the EM objective of lower BESS degradation. The behaviour of SCR and BESS degradation tend to be complementary. In the practical scenario SCR falls lower than the ideal predictive management unit. This is expected due to the errors in prediction, which results in some usable power from the PV generation not utilised and being send to the grid. Nevertheless, it should be noted that the SCR in the practical scenario is still not very low in comparison to the conventional scheme at 52.71% which is 96.5% the maximum possible value. This value was achieved despite higher error in PV prediction due to absence of weather data. The availability of this data will only improve the prediction accuracy and improve SCR. This highlights the economic suitability of predictive management in practical scenarios where uncertainty in forecast exists.

2) *Feed-in power limitation assessment*: The Table.II also shows the annual PV power curtailment (due to high grid feed-in power) with each management scheme. The conventional method due to early BESS full charging requires has maximum annual power curtailment of 542.5kW. In contrast the ideal MPC, with perfect forecast, manages PV BESS operation with zero curtailment. In event of forecast error, as shown in Fig.9 peak power feed-in occurs and as such the need for curtailment. Nevertheless, as shown in Table.II the PV power curtailed is only 34.91 kW which is almost 94% lesser than conventional method. This highlights increased utilisation of PV power with PEMS.

3) *Battery degradation assessment*: The BESS degradation with different strategies is shown in Table.II. The degradation can be better explained with Fig.11, Fig.12 which shows the cycling and SOC dwell times of the BESS respectively. The plot in Fig.11 was generated from BESS SOC profile using rainflow algorithm. The x-axis of Fig.11 indicate half of the cycle magnitude whereas the y-axis indicates the mean SOC value of a cycle. For example, if BESS cycles between 10-90% SOC, the x and y-axis values will be 45.

The conventional strategy exhibits the highest BESS degradation while predictive strategies (ideal and practical case) show almost a 6% reduction in annual BESS degradation. The early BESS charging in the conventional scheme results

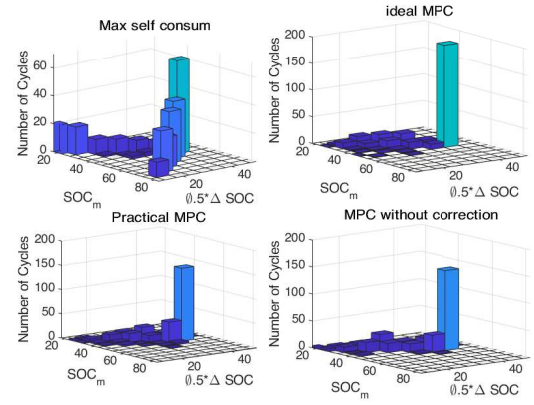


Fig. 11: BESS cycling undergone with different energy management schemes.

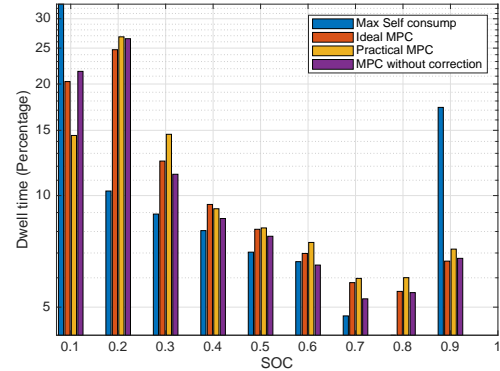


Fig. 12: BESS cycling undergone with different energy management schemes.

in increased dwell times at high SOC levels as shown in Fig.12, causing calendar ageing. However high SOC dwell times and calendar ageing is significantly reduced in predictive strategies, due to shifting of the BESS charging to peak generation period. The predictive strategies however exhibit higher cycling (Fig.11) and therefore should have higher cycling ageing in comparison to conventional scheme. Nevertheless, the improvement in calendar ageing outweighs this effect.

The annual degradation in BESS for the ideal and practical case is very similar. Assessing the cycling plot in Fig.11 it can be observed that the ideal MPC case undergoes a higher number of large magnitude cycles in comparison to the practical case. In comparison, the practical case has larger dwell times at high SOC levels due to earlier charging of BESS compared to ideal case. Therefore the combined effect of the both leads to similar degradation in both cases of PEMS.

Finally, an analysis of constraint tightening's effect on the objectives considered in the PEMS is carried out. The performance of PEMS without the tightening (but with imperfect forecast) is shown in Fig.9,10, 11, 12, as MPC without correction. Based on Fig.10 the grid feed-in performance in MPC with and without constraint tightening appears similar. However assessing Table.II it can be seen that, without constraint tightening, the annual grid feed-in curtailment tend to be higher whereas the SCR tends to be better. This is due to the conservative nature of decision making of PEMS due to constraint tightening. The PEMS expects a deviation in forecast value and as such prevents the BESS from charging or

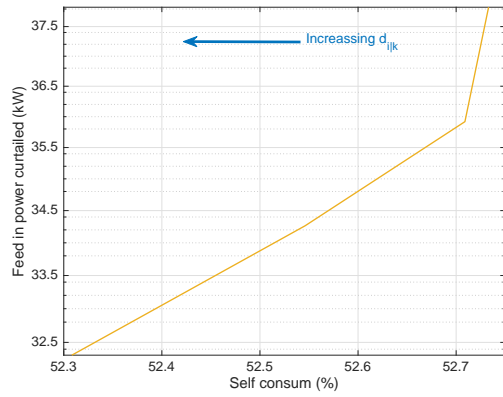


Fig. 13: Variation of feed in curtailment and self consumption with increasing uncertainty bound ($d_{i|k}$) on forecast values.

discharging excessively. This leads to some usable PV power being sent to grid, thus lowering SCR. This also results in BESS from not being fully charged at peak generation time thereby limiting grid feed-in curtailment. Therefore increasing the bounds on uncertainty and the resulting increase in constraint tightening always reduces the feed-in curtailment but at the cost of lower SCR as shown in Fig.13. The annual BESS degradation is also lesser without constraint tightening as shown in Table.II. This is also a result of the conservative decision making of PEMS which results in the BESS having a increased dwell times at higher SOC levels as evident from Fig.12. These results also justify the use of mean absolute aggregated error in the prediction window for defining the bounds $d_{i|k}$ instead of utilising the mean aggregated error at every point in the prediction window. This is because utilising the point wise error would have resulted in higher bounds in $d_{i|k}$, considering the bigger error in PV forecast, leading to very conservative decision making.

IV. CONCLUSION

The PEMS in PV-BESS is capable of improving the grid congestion and BESS degradation performance in comparison to the conventional scheme. However it is achieved at a cost of slight reduction of SCR. The error in predicted generation and load profiles are always going to reduce the SCR when using forecast based methods, unless a perfect forecast can be achieved. Nevertheless, as shown in this work online scheduling using MPC with good forecasting does not significantly reduce the SCR. It should also be noted even though forecast of PV generation was done without the weather data the online nature of MPC allowed better decision making.

REFERENCES

- [1] H. Schermeyer, M. Studer, M. Ruppert, and W. Fichtner, "Understanding distribution grid congestion caused by electricity generation from renewables," in *Smart Energy Research. At the Crossroads of Engineering, Economics, and Computer Science*. Springer, 2017, pp. 78–89.
- [2] K. Divya and J. Østergaard, "Battery energy storage technology for power systems—an overview," *Electric power systems research*, vol. 79, no. 4, pp. 511–520, 2009.
- [3] J. Moshövel, K.-P. Kairies, D. Magnor, M. Leuthold, M. Bost, S. Gähns, E. Szczechowicz, M. Cramer, and D. U. Sauer, "Analysis of the maximal possible grid relief from pv-peak-power impacts by using storage systems for increased self-consumption," *Applied Energy*, vol. 137, pp. 567–575, 2015.

- [4] G. Angenendt, S. Zurmühlen, H. Axelsen, and D. U. Sauer, "Comparison of different operation strategies for pv battery home storage systems including forecast-based operation strategies," *Applied energy*, vol. 229, pp. 884–899, 2018.
- [5] J. Vetter, P. Novák, M. R. Wagner, C. Veit, K.-C. Möller, J. Besenhard, M. Winter, M. Wohlfahrt-Mehrens, C. Vogler, and A. Hammouche, "Ageing mechanisms in lithium-ion batteries," *Journal of power sources*, vol. 147, no. 1-2, pp. 269–281, 2005.
- [6] F. Garcia-Torres and C. Bordons, "Optimal economical schedule of hydrogen-based microgrids with hybrid storage using model predictive control," *IEEE Transactions on Industrial Electronics*, vol. 62, no. 8, pp. 5195–5207, 2015.
- [7] A. Parisio, E. Rikos, and L. Glielmo, "A model predictive control approach to microgrid operation optimization," *IEEE Transactions on Control Systems Technology*, vol. 22, no. 5, pp. 1813–1827, 2014.
- [8] J. Li and M. A. Danzer, "Optimal charge control strategies for stationary photovoltaic battery systems," *Journal of Power Sources*, vol. 258, pp. 365–373, 2014.
- [9] M. Schneider, P. Boras, H. Schaefer, L. Quurck, and S. Rinderknecht, "Effects of operational strategies on performance and costs of electric energy storage systems," *Energy Procedia*, vol. 46, pp. 271–280, 2014.
- [10] B. Kouvaritakis and M. Cannon, "Model predictive control," *Switzerland: Springer International Publishing*, 2016.
- [11] A. Cecilia, J. Carroquino, V. Roda, R. Costa-Castelló, and F. Bareras, "Optimal energy management in a standalone microgrid, with photovoltaic generation, short-term storage, and hydrogen production," *Energies*, vol. 13, no. 6, p. 1454, Mar. 2020.
- [12] C. Bordons, F. Garcia-Torres, and M. R. Carlini, "Model predictive control of interconnected microgrids and with electric vehicles," *Revista Iberoamericana de Automática e Informática industrial*, 2020.
- [13] J. M. Maciejowski, *Predictive control: with constraints*. Pearson education, 2002.
- [14] S. Haykin, *Neural networks: a comprehensive foundation*. Prentice Hall PTR, 1994.
- [15] M. Abdel-Nasser and K. Mahmoud, "Accurate photovoltaic power forecasting models using deep lstm-rnn," *Neural Computing and Applications*, vol. 31, no. 7, pp. 2727–2740, 2019.
- [16] H. Shi, M. Xu, and R. Li, "Deep learning for household load forecasting—a novel pooling deep rnn," *IEEE Transactions on Smart Grid*, vol. 9, no. 5, pp. 5271–5280, 2017.
- [17] A. Fadhilah, S. Suriawati, H. Amir, Z. Izham, and S. Mahendran, "Malaysian day-type load forecasting," in *2009 3rd International Conference on Energy and Environment (ICEE)*. IEEE, 2009, pp. 408–411.
- [18] V. Nair and G. E. Hinton, "Rectified linear units improve restricted boltzmann machines," in *Proceedings of the 27th international conference on machine learning (ICML-10)*, 2010, pp. 807–814.
- [19] S. S. Haykin et al., *Neural networks and learning machines/Simon Haykin*. New York: Prentice Hall, 2009.
- [20] J. W. Chinneck, "Practical optimization: a gentle introduction," *Systems and Computer Engineering*, Carleton University, Ottawa. <http://www.sce.carleton.ca/faculty/chinneck/po.html>, 2006.
- [21] E. C. Kerrigan and J. M. Maciejowski, "Soft constraints and exact penalty functions in model predictive control," 2000.
- [22] L. Gurobi Optimization, "Gurobi optimizer reference manual," 2019. [Online]. Available: <http://www.gurobi.com>
- [23] A. Richards and J. How, "Robust stable model predictive control with constraint tightening," in *2006 American Control Conference*. IEEE, 2006, pp. 6–pp.
- [24] D. L. Marino, K. Amarasinghe, and M. Manic, "Building energy load forecasting using deep neural networks," in *IECON 2016-42nd Annual Conference of the IEEE Industrial Electronics Society*. IEEE, 2016, pp. 7046–7051.
- [25] T. Stetz, F. Marten, and M. Braun, "Improved low voltage grid-integration of photovoltaic systems in germany," *IEEE Transactions on sustainable energy*, vol. 4, no. 2, pp. 534–542, 2012.
- [26] M. Bost, B. Hirschl, and A. Aretz, *Effekte von Eigenverbrauch und Netzparität bei der Photovoltaik*. Institut für ökologische Wirtschaftsforschung (IÖW) GmbH, gemeinnützig, 2011.
- [27] F. Chollet et al., "Keras," <https://keras.io>, 2015.
- [28] D. P. Kingma and J. Ba, "Adam: A method for stochastic optimization," *arXiv preprint arXiv:1412.6980*, 2014.
- [29] L. Prechelt, "Automatic early stopping using cross validation: quantifying the criteria," *Neural Networks*, vol. 11, no. 4, pp. 761–767, 1998.